

# $\alpha$ -B Crystallin Reverses High Diastolic Stiffness of Failing Human Cardiomyocytes

Constantijn Franssen, MD; Jeroen Kole, BAsc; René Musters, PhD; Nazha Hamdani, PhD; Walter J. Paulus, MD, PhD

**Background**—Cardiomyocytes with a less distensible titin and interstitial collagen contribute to the high diastolic stiffness of failing myocardium. Their relative contributions and mechanisms underlying loss of titin distensibility were assessed in failing human hearts.

**Methods and Results**—Left ventricular tissue was procured in patients with aortic stenosis (AS, n=9) and dilated cardiomyopathy (DCM, n=6). Explanted donor hearts (n=8) served as controls. Stretches were performed in myocardial strips, and an extraction protocol differentiated between passive tension ( $F_{\text{passive}}$ ) attributable to cardiomyocytes or to collagen.  $F_{\text{passive}}$ -cardiomyocytes was higher in AS and DCM at shorter muscle lengths, whereas  $F_{\text{passive}}$ -collagen was higher in AS at longer muscle lengths and in DCM at shorter and longer muscle lengths. Cardiomyocytes were stretched to investigate titin distensibility. Cardiomyocytes were incubated with alkaline phosphatase, subsequently reassessed after a period of prestretch and finally treated with the heat shock protein  $\alpha$ -B crystallin. Alkaline phosphatase shifted the  $F_{\text{passive}}$ -sarcomere length relation upward only in donor. Prestretch shifted the  $F_{\text{passive}}$ -sarcomere length relation further upward in donor and upward in AS and DCM.  $\alpha$ -B crystallin shifted the  $F_{\text{passive}}$ -sarcomere length relation downward to baseline in donor and to lower than baseline in AS and DCM. In failing myocardium, confocal laser microscopy revealed  $\alpha$ -B crystallin in subsarcolemmal aggregates.

**Conclusions**—High cardiomyocyte stiffness contributed to stiffness of failing human myocardium because of reduced titin distensibility. The latter resulted from an absent stiffness-lowering effect of baseline phosphorylation and from titin aggregation. High cardiomyocyte stiffness was corrected by  $\alpha$ -B crystallin probably through relief of titin aggregation. (*Circ Heart Fail.* 2017;10:e003626. DOI: 10.1161/CIRCHEARTFAILURE.116.003626.)

**Key Words:** aortic valve stenosis ■ collagen ■ diastole ■ extracellular matrix ■ heat shock proteins

High diastolic stiffness of failing human myocardium results from raised diastolic stiffness of cardiomyocytes and from excessive deposition of collagen.<sup>1</sup> Raised diastolic stiffness of cardiomyocytes has been reported in several heart failure phenotypes such as heart failure with preserved ejection (HFPEF),<sup>2</sup> heart failure with reduced ejection fraction,<sup>3</sup> or aortic valve stenosis (AS).<sup>4</sup> Several issues concerning the raised diastolic stiffness of failing human cardiomyocytes remain incompletely understood and are addressed in the present study. These issues are (1) Does raised diastolic stiffness of failing human cardiomyocytes contribute to the overall myocardial stiffness? (2) Which modifications of titin, the giant cytoskeletal protein responsible for cardiomyocyte stiffness, account for the high intrinsic stiffness of failing human cardiomyocytes; and (3) How can they be corrected?

## See Clinical Perspective

Because of parallel alignment of cardiomyocytes and extracellular matrix, overall myocardial stiffness tracks stiffness of

the most severely affected compartment. Raised cardiomyocyte stiffness will, therefore, contribute less to myocardial stiffness in the presence of severe myocardial fibrosis. Using a myofibrillary extraction technique and isolated left ventricular (LV) myocardial muscle strips,<sup>5</sup> the relative contributions of cardiomyocyte and extracellular matrix stiffness have been assessed in mice after transverse aortic constriction<sup>6</sup>, in mice with a knock-out of immunoglobulin-like domains of titin (Ig-KO),<sup>7</sup> in ZSF1 rats with HFPEF,<sup>8</sup> in dilated cardiomyopathy (DCM)<sup>9</sup> patients, and in HFPEF patients with coronary artery disease<sup>10</sup>. In transverse aortic constriction mice, in DCM patients with low N2BA/N2B titin isoform ratio, and in HFPEF patients with coronary artery disease, both titin and collagen contributed to overall myocardial stiffness with equalization of their respective contributions at the outer limit of physiological sarcomere lengths (SLs), whereas in Ig-KO mice and ZSF1-HFPEF rats, titin remained the main determinant of overall myocardial stiffness even at the outer limit of physiological sarcomere lengths. The present study extends

Received July 5, 2016; accepted January 23, 2017.

From the Department of Physiology, Institute for Cardiovascular Research, VU University Medical Center, Amsterdam, The Netherlands (C.F., J.K., R.M., N.H., W.J.P.); and Department of Cardiovascular Physiology, Ruhr University Bochum, Germany (N.H.).

Correspondence to Walter J. Paulus, MD, PhD, Institute for Cardiovascular Research, VU University Medical Center, Van der Boerhorststraat 7, 1081 BT Amsterdam, The Netherlands. E-mail wj.paulus@vumc.nl

© 2017 American Heart Association, Inc.

*Circ Heart Fail* is available at <http://circheartfailure.ahajournals.org>

DOI: 10.1161/CIRCHEARTFAILURE.116.003626

these observations to clinical heart failure by examining LV myocardial muscle strips procured from patients without coronary artery disease experiencing either DCM or AS.

Raised diastolic stiffness of failing human cardiomyocytes was hitherto mainly attributed to post-translational modifications of titin consisting of lack or excess phosphorylation at specific sites along the titin molecule.<sup>11,12</sup> Recently, altered diastolic stiffness was suggested to also originate from titin being damaged by oxidative or physical stress.<sup>13,14</sup> S-glutathionylated cryptic cysteines of immunoglobulin domains were shown to decrease mechanical stability and refolding ability of titin.<sup>14</sup> Furthermore, previous exposure of cardiomyocytes to stretch and low pH caused a rise of cardiomyocyte stiffness, which was suppressed by small heat shock proteins such as HSP27 and  $\alpha$ -B crystallin.<sup>15</sup> The protective role of  $\alpha$ -B crystallin on titin distensibility was also evident from earlier studies in which  $\alpha$ -B crystallin lowered the persistence length of the N2B-U segment and reduced the unfolding probability of the immunoglobulin domains flanking the N2B-U segment.<sup>16</sup> The relative importance of deranged phosphorylation and structural damage of titin for diastolic stiffness of failing human cardiomyocytes is currently unclear and therefore is also addressed in the present study.

## Methods

### Human Samples

AS patients (n=9) had symptomatic, severe AS without concomitant coronary artery disease. Biopsy specimens from this group were procured from endomyocardial tissue resected from the septum (Morrow procedure) during aortic valve replacement. DCM specimens were procured from LV biopsies (n=3) or from explanted hearts from end-stage heart failure patients (n=3). DCM patients had no significant coronary stenosis, and their biopsies showed no inflammation or infiltration. Control samples were obtained from explanted donor hearts (n=8). The local ethics committee approved the study protocol. Written informed consent was obtained from all patients. Clinical characteristics and hemodynamic data of the different patient groups are shown in Table.

### Force Measurements in Small Muscle Strips

Small muscle strips (150–450  $\mu$ m in diameter and 800–1900  $\mu$ m in length) were dissected from myocardial samples (n=24 for AS; n=16 for DCM; n=20 for donor). After incubation for 1 hour in relaxing solution supplemented with 0.2% Triton X-100 to remove all membrane structures, strips were attached between a force transducer and length motor in a relaxing solution (in mmol/L: free Mg, 1; KCl, 100; EGTA, 2; Mg-ATP, 4; imidazole, 10; pH 7.0). Strips were gently stretched till slack length, that is, the minimal length at which passive tension ( $F_{\text{passive}}$ ) is being build up. As a test of cell viability, each muscle strip was transferred from relaxing to maximally activating solution (pCa4.5), at which isometric force developed. After stabilization for 5 minutes in relaxing solution, strips were stretched to 10%, 15%, 20%, and 25% length relative to slack length with return to slack length in between each lengthening step.  $F_{\text{passive}}$  was measured at each stage of muscle strain.

Subsequently, thick and thin filaments were extracted by immersing the preparation in relaxing solution containing 0.6 mol/L KCl (45 minutes at 20°C) followed by relaxing solution containing 1.0 mol/L KI (45 minutes at 20°C).<sup>5,8,10</sup> After the extraction procedure, the muscle bundles were stretched again, and the  $F_{\text{passive}}$  remaining after KCl/KI treatment was ascribed to the extracellular matrix. At each stage of muscle strain,  $F_{\text{passive}}$  after extraction was subtracted from baseline value to yield  $F_{\text{passive}}$  attributable to cardiomyocyte stiffness or titin.

### Force Measurements in Isolated Cardiomyocytes

Force measurements were performed on single demembrated cardiomyocytes (n ranged from 9 to 15 for each group and experimental protocol). Cardiomyocytes were isolated from donor, AS, and DCM hearts. Briefly, samples were defrozed in relaxing solution (in mmol/L: free Mg, 1; KCl, 100; EGTA, 2; Mg-ATP, 4; imidazole, 10; pH 7.0), mechanically disrupted, and incubated for 5 minutes in relaxing solution supplemented with 0.5% Triton X-100. The cell suspension was washed 5 times in relaxing solution. Single cardiomyocytes were selected under an inverted microscope and attached with silicone adhesive between a force transducer and a piezoelectric motor. Cardiomyocyte  $F_{\text{passive}}$  was measured in relaxing buffer at room temperature within a SL range between 1.8 and 2.4  $\mu$ m. The stretch protocol consisted of an uninterrupted stepwise increase in SL without return to slack length.<sup>14,15</sup> Force values were normalized to cardiomyocyte cross-sectional area calculated from the diameter of the cells, assuming a cylindrical shape. As a test of cell viability, each cardiomyocyte was also transferred from relaxing to maximally activating solution (pCa4.5), at which isometric force developed. Once a steady-state force was reached, the cell was shortened within 1 ms to 80% of its original length to determine baseline force. Only cells developing active forces >20 mN/mm<sup>2</sup> were included in the analysis. Thereafter, cardiomyocytes were incubated in relaxing solution supplemented with alkaline phosphatases (AP; 0.2 U/ $\mu$ L; New England Biolabs), 6 mmol/L dithiothreitol (MP Biochemicals) for 40 minutes at room temperature, and  $F_{\text{passive}}$  was measured at SL 1.8 to 2.4  $\mu$ m. The stretch protocol again consisted of an uninterrupted stepwise increase in SL without return to slack length.<sup>14,15</sup> Subsequently, cardiomyocytes were stretched to  $\approx$ 2.6  $\mu$ m SL, incubated in relaxing buffer with pH 6.6, and held in the stretched state for 15 minutes (prestretch). Thereafter, cardiomyocytes were returned to slack length and stabilized for 5 minutes before recording the  $F_{\text{passive}}$  with an identical stretch protocol from SL 1.8 to 2.4  $\mu$ m in the low pH buffer. Finally, the pH 6.6 buffer was supplemented with recombinant human  $\alpha$ -B crystallin at 0.1 mg/mL, and  $F_{\text{passive}}$  was measured in the presence of  $\alpha$ -B crystallin again at SL 1.8 to 2.4  $\mu$ m with an identical stretch protocol. In a second set of experiments, single AS cardiomyocytes underwent either incubation at pH 6.6 alone or a prestretch in relaxing buffer with pH 6.6 to an approximate SL 2.6  $\mu$ m, followed by the same stretch protocol from SL 1.8 to 2.4  $\mu$ m. Finally, in a third set of experiments,  $F_{\text{passive}}$  was measured in single AS cardiomyocytes from SL 1.8 to 2.4  $\mu$ m before and after incubation with  $\alpha$ -B crystallin, before and after incubation with  $\alpha$ -B crystallin and a prestretch to an approximate SL 2.6  $\mu$ m, and before and after incubation with  $\alpha$ -B crystallin, a prestretch to  $\approx$ 2.6  $\mu$ m SL and incubation at pH 6.6.

### Immunofluorescence Staining and Confocal Scanning Laser Microscopy

Frozen human heart tissue was sectioned to a thickness of 5  $\mu$ m using a cryostat (Leica). The sections were fixed with 3% paraformaldehyde, permeabilized with 0.05% Tween 20 and immunostained using goat anti- $\alpha$ -B crystallin (Santa Cruz) diluted 1 in 100 in PBS+1% BSA (immunohistochemical grade; Vector Laboratories). Antigoat conjugated to Alexa 555 (ThermoFisher) was used to visualize  $\alpha$ -B crystallin. Membranes were stained using WGA conjugated with Alexa 647 (ThermoFisher) diluted 1 in 100 in PBS. Nuclei were visualized using Picogreen reagent (ThermoFisher) diluted 1 in 10000 in PBS. Confocal scanning laser microscopy was performed on a Leica TCS SP8 STED 3X (Leica Microsystems). Picogreen, Alexa 555, and Alexa 647 were irradiated with a pulsed white light laser at 502, 553, and 631 nm, respectively. A 63 $\times$  oil objective with NA 1.4 Numerical Aperture was used to image the sample. Detection of the fluorescent signal was performed with gated Hybrid Detectors. Finally, the images were deconvolved using Huygens Professional (Scientific Volume Imaging).

### Statistical Analysis

Comparisons between DCM and donor and between AS and donor were analyzed using ANOVA followed by a multiple comparison procedure (Bonferroni). Differences within groups were measured by

**Table. Baseline Characteristics and Hemodynamics of Patients**

|                                 | Donors | AS        | DCM       | P Value (Donors vs AS) | P Value (Donors vs DCM) |
|---------------------------------|--------|-----------|-----------|------------------------|-------------------------|
| Age, y                          | 51±4   | 65.3±1.6  | 60.0±2.1  | <0.0001                | <0.0001                 |
| Male sex, %                     | 25     | 47        | 70        | <0.0001                | <0.0001                 |
| Hypertension, %                 | ...    | 58        | 16        |                        |                         |
| DM, %                           | ...    | 26        | 30        |                        |                         |
| BMI, kg/m <sup>2</sup>          | ...    | 28.1±0.6  | 27.5±0.8  |                        |                         |
| GFR, mL/min/1.73 m <sup>2</sup> | ...    | 68.9±18.5 | 63.5±15.7 |                        |                         |
| Atrial fibrillation, %          | ...    | 2         | 33        |                        |                         |
| Medication, %                   |        |           |           |                        |                         |
| ACE-I/ARB                       | ...    | 43        | 81        |                        |                         |
| $\beta$ -Blocker                | ...    | 61        | 63        |                        |                         |
| Diuretic                        | ...    | 54        | 72        |                        |                         |
| Aldosterone receptor antagonist | ...    | 7         | 74        |                        |                         |
| Digoxin                         | ...    | 2         | 33        |                        |                         |
| Statin                          | ...    | 46        | 21        |                        |                         |
| Metformin                       | ...    | 3         | 14        |                        |                         |
| Bronchodilators                 | ...    | 9         | 19        |                        |                         |
| Hemodynamics                    |        |           |           |                        |                         |
| HR, beats per min               | 80±16  | 74±2      | 82±4      | 0.0035                 | 0.4674                  |
| LVPSP, mm Hg                    | 135±15 | 223±4     | 120±3     | <0.0001                | <0.0001                 |
| LVEDP, mm Hg                    | 13±4   | 22.8±1.4  | 22.3±1.4  | <0.0001                | <0.0001                 |
| LVEDVI, mL/m <sup>2</sup>       | 78±23  | 55±2      | 127±5     | <0.0001                | <0.0001                 |
| LVEF, %                         | 73±3   | 64.0±1.2  | 29.4±1.5  | <0.0001                | <0.0001                 |

Values are mean±SD or %.

ACE-I indicates angiotensin-converting enzyme inhibitor; ARB, angiotensin II receptor blocker; AS, aortic stenosis; BMI, body mass index; DCM, dilated cardiomyopathy; DM, diabetes mellitus; GFR, glomerular filtration rate; HR, heart rate; LVEDP, left ventricular end-diastolic pressure; LVEDVI, left ventricular end-diastolic volume index; LVEF, left ventricular ejection fraction; and LVPSP, left ventricular peak systolic pressure.

repeated-measures ANOVA. A 2-tailed test with a *P* value <0.05 was considered significant. All analyses were performed using Prism software (GraphPad Software Inc, version 6.0).

## Results

### Force Measurements in Muscle Strips

Initial stretches with intact muscle strips, in which both cardiomyocytes and extracellular matrix contribute to  $F_{\text{passive}}$ ,

showed that DCM and AS strips developed higher forces during all stretches compared with donor (Figure 1A). The extraction protocol decreased  $F_{\text{passive}}$  in all groups (Figure 1B).  $F_{\text{passive}}$  caused by extracellular matrix stiffness was higher in DCM strips than in donors for stretches ranging from 10% to 20% slack length (Figure 2).  $F_{\text{passive}}$  caused by extracellular matrix was higher in AS than in donors for stretches exceeding 20% slack length (Figure 2).  $F_{\text{passive}}$

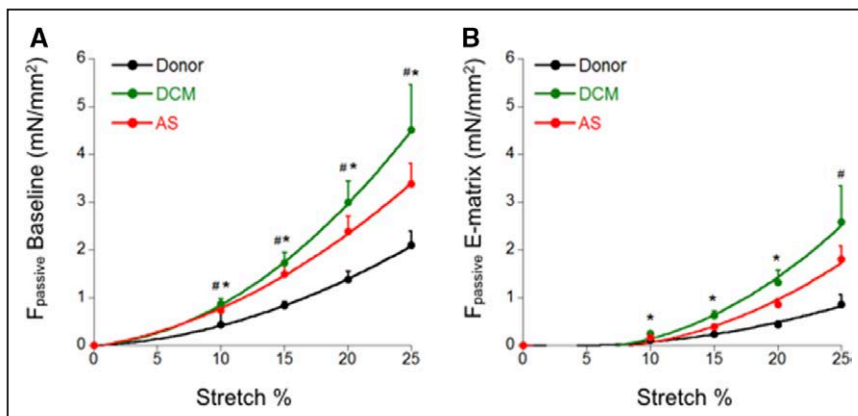


**Figure 1.**  $F_{\text{passive}}$  in myocardial strips. At baseline,  $F_{\text{passive}}$  was significantly higher in dilated cardiomyopathy (DCM) and aortic stenosis (AS) strips compared with donor (A). After extracting thick and thin filaments, the remaining  $F_{\text{passive}}$  can be attributed to the extracellular matrix (E-matrix; B). \**P*<0.05 DCM vs donor; #*P*<0.05 AS vs donor.

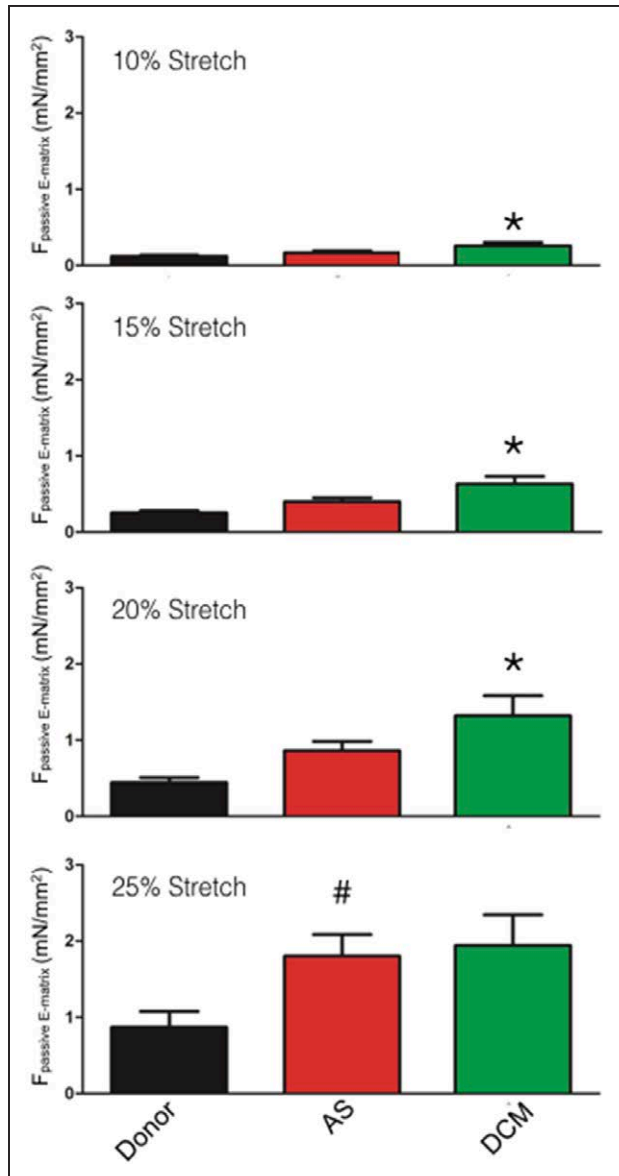


**Figure 2.**  $F_{\text{passive}}$  caused by the extracellular matrix (E-matrix). Aortic stenosis (AS) strips had significantly higher E-matrix-based  $F_{\text{passive}}$  than donor when stretched to 25% slack length. Dilated cardiomyopathy (DCM) strips had significantly higher E-matrix-based  $F_{\text{passive}}$  for stretches ranging from 10% to 20% slack length. \* $P < 0.05$  DCM vs donor; # $P < 0.05$  AS vs donor.

caused by cardiomyocyte stiffness, which is attributable to titin, was higher in DCM than in donors for stretches ranging from 10% to 20% slack length and higher in AS than in donors for stretches ranging from 10% to 15% slack length (Figure 3).

The higher  $F_{\text{passive}}$  caused by cardiomyocyte stiffness cannot be explained by isoform shifts of titin because both DCM and AS express more of the compliant N2BA titin isoform.<sup>3,4,17</sup> To further analyze the difference in  $F_{\text{passive}}$  related to cardiomyocytes, we subjected isolated cardiomyocytes (1) to treatment with AP to discern the contribution of titin phosphorylation and (2) to conditions prevailing in failing myocardium such as high stretch and hypoperfusion-related acidosis.<sup>15</sup>

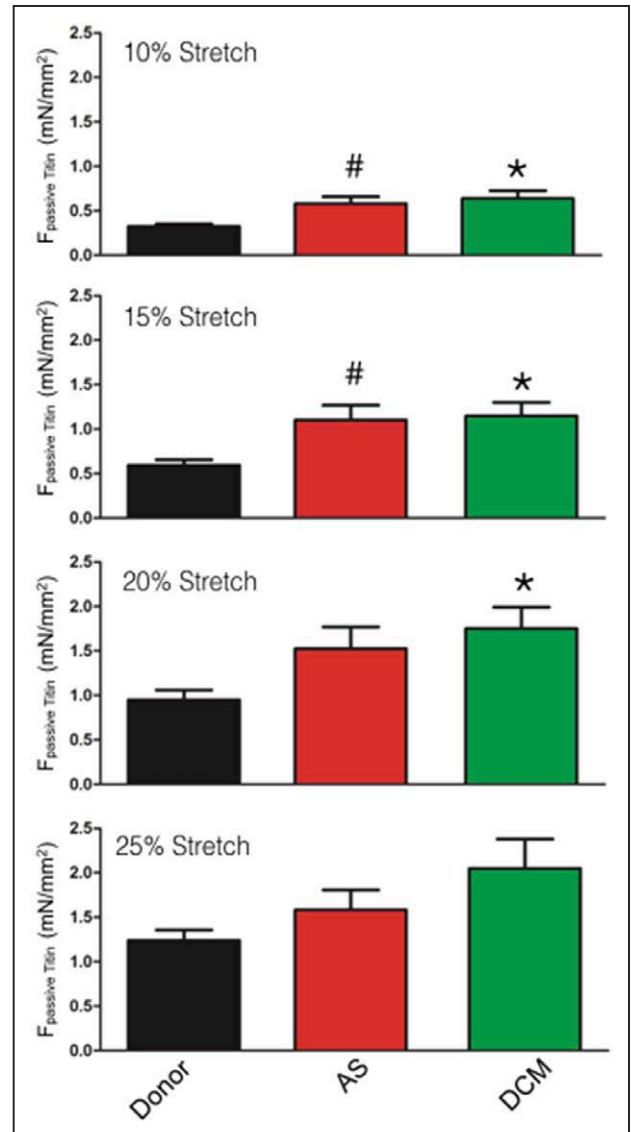


**Figure 3.**  $F_{\text{passive}}$  caused by titin. In aortic stenosis (AS) strips, titin-based  $F_{\text{passive}}$  was higher than in donor strips for stretches ranging from 10% to 15% slack length. In dilated cardiomyopathy (DCM) strips, titin-based  $F_{\text{passive}}$  was higher than in donor for stretches ranging from 10% to 20% slack length. \* $P < 0.05$  DCM vs donor; # $P < 0.05$  AS vs donor.

### Force Measurements in Isolated Cardiomyocytes

In donor cardiomyocytes (Figure 4A), the  $F_{\text{passive}}$ -SL curve shifted upward after administration of AP, which dephosphorylates titin. In contrast, the  $F_{\text{passive}}$ -SL curve failed to shift in AS and DCM cardiomyocytes (Figure 4B and 4C). This suggests that previous *in vivo* phosphorylation status did not correct high stiffness of AS and DCM cardiomyocytes. The  $F_{\text{passive}}$ -SL curve of donor cardiomyocytes after AP was still lower ( $P < 0.05$ ) than the  $F_{\text{passive}}$ -SL curve after AP in AS and DCM cardiomyocytes. Mechanisms other than phosphorylation status therefore contribute to the high diastolic stiffness of AS and DCM cardiomyocytes. The effects of prestretch and acidic pH were subsequently investigated. The  $F_{\text{passive}}$ -SL curve shifted further upward in donor cardiomyocytes after performing a prestretch and imposing an acidic pH. After

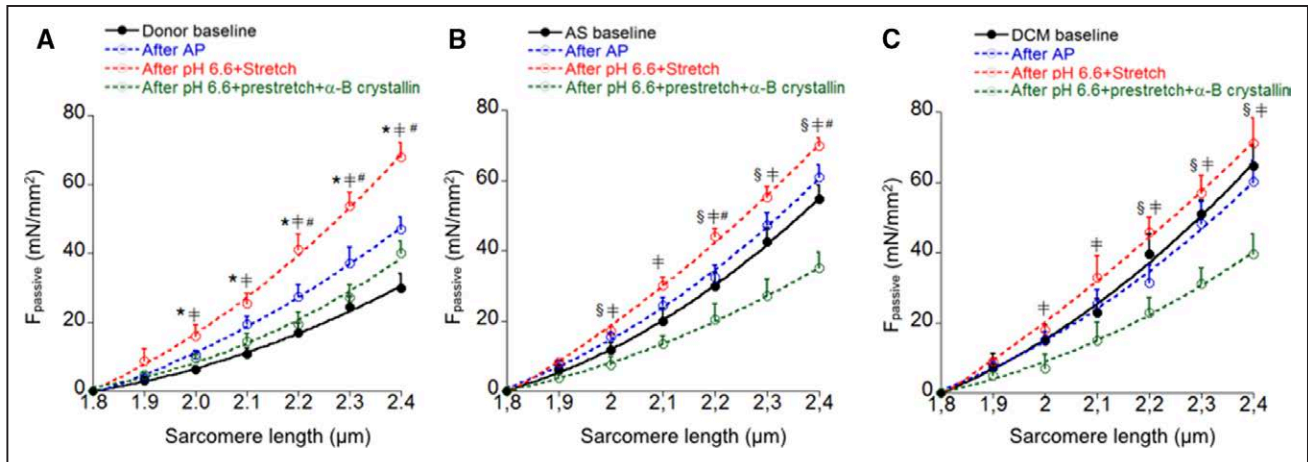


**Figure 4.**  $F_{\text{passive}}$  in single myocytes. **A**, In donor cardiomyocytes,  $F_{\text{passive}}$  significantly increased after administration of alkaline phosphatase (AP) and increased further after performing a prestretch in an acidic environment. After in vitro administration of  $\alpha$ -B crystallin,  $F_{\text{passive}}$  fell to a position slightly lower than after AP. **B**, In AS cardiomyocytes, no significant change in  $F_{\text{passive}}$  was observed after incubation with AP. After the prestretch in pH 6.6,  $F_{\text{passive}}$  increased significantly compared with baseline, but in vitro treatment with  $\alpha$ -B crystallin lowered  $F_{\text{passive}}$  to a level significantly lower than baseline. **C**, In dilated cardiomyopathy (DCM) cardiomyocytes, incubation with AP had no effect on  $F_{\text{passive}}$ , but performing a prestretch in an acidic environment significantly increased passive stiffness. After in vitro treatment with  $\alpha$ -B crystallin,  $F_{\text{passive}}$  fell to a level significantly below baseline. \* $P < 0.05$  AP vs baseline; # $P < 0.05$  pH 6.6+prestretch vs AP; § $P < 0.05$   $\alpha$ -B crystallin vs pH 6.6+prestretch; § $P < 0.05$   $\alpha$ -B crystallin vs baseline.

administration of  $\alpha$ -B crystallin, the curve returned to a position slightly lower than after AP.

In AS cardiomyocytes (Figure 4B), no significant change in the  $F_{\text{passive}}$ -SL curve was observed after incubation with AP. After imposition of prestretch and pH 6.6, the  $F_{\text{passive}}$ -SL curve shifted upward compared with baseline. After treatment with  $\alpha$ -B crystallin, the  $F_{\text{passive}}$ -SL curve fell to a position that was significantly lower than baseline and comparable to the baseline position of donor cardiomyocytes. This finding implies presence at baseline of previous stretch- and pH-induced changes in AS myocardium, which could be corrected by administration of  $\alpha$ -B crystallin.

The same series of experiments in single DCM cardiomyocytes showed similar findings (Figure 4C) as in AS cardiomyocytes: incubation with AP had no effect on the  $F_{\text{passive}}$ -SL curve but performing a prestretch in an acidic environment shifted the curve significantly upward. After in vitro treatment with  $\alpha$ -B crystallin, the  $F_{\text{passive}}$ -SL curve fell to a position that was significantly below baseline and comparable to the baseline position of donor cardiomyocytes. This again implies presence at baseline of previous stretch- and pH-induced changes in DCM cardiomyocytes, which could be corrected by administration of  $\alpha$ -B crystallin.

### Effects of Prestretch, pH, and $\alpha$ -B Crystallin in Single AS Cardiomyocytes

The relative importance of prestretch and pH 6.6 were analyzed in single AS cardiomyocytes. In the absence of previous administration of AP, lowering the pH to 6.6 had no effect on  $F_{\text{passive}}$  (Figure 5A), but addition of a prestretch to  $\approx 2.6$   $\mu\text{m}$  SL significantly shifted the  $F_{\text{passive}}$ -SL curve upward (Figure 5B). Incubation with  $\alpha$ -B crystallin shifted the  $F_{\text{passive}}$ -SL curve significantly downward compared with baseline (Figure 6A). Incubation with  $\alpha$ -B crystallin shifted the  $F_{\text{passive}}$ -SL curve to a similar position after prestretch or prestretch in combination with pH 6.6 (Figure 6B and 6C).

### Immunofluorescence Staining and Confocal Scanning Laser Microscopy

Confocal laser microscopical images were obtained from LV myocardium of donor and AS patients with immunohistochemical visualization of cell membranes, nuclei, and  $\alpha$ -B crystallin (Figure 7). In myocardium of AS patients, intensity of  $\alpha$ -B crystallin expression was higher than in donor with appearance of  $\alpha$ -B crystallin-containing aggregates<sup>18</sup> (Figure 7), which were especially prominent in the subsarcolemma close to the capillaries (white arrows in Figure 7). The latter suggests signals originating from the microvascular endothelium to be involved in the subsarcolemmal mobilization of  $\alpha$ -B crystallin in failing cardiomyocytes.

### Discussion

The present study investigated high diastolic stiffness of failing human myocardial strips and cardiomyocytes and observed the following: (1) high diastolic stiffness of cardiomyocytes significantly contributes to the overall stiffness of LV myocardial strips of AS and DCM patients; (2) dephosphorylation with AP shifts the diastolic  $F_{\text{passive}}$ -SL relation upward in donor but not in AS or DCM cardiomyocytes; (3) after dephosphorylation, exposure to prestretch causes an upward shift of the diastolic  $F_{\text{passive}}$ -SL relations in AS and DCM cardiomyocytes and a further upward shift of the diastolic  $F_{\text{passive}}$ -SL relation in donor cardiomyocytes; (4) subsequent administration of  $\alpha$ -B crystallin shifts the diastolic  $F_{\text{passive}}$ -SL relations downward in donor, AS, and DCM cardiomyocytes to a position that coincides with the baseline diastolic  $F_{\text{passive}}$ -SL relation of donor cardiomyocytes. This finding is consistent with  $\alpha$ -B crystallin, providing protection against stretch-induced damage to titin in failing AS and DCM cardiomyocytes.

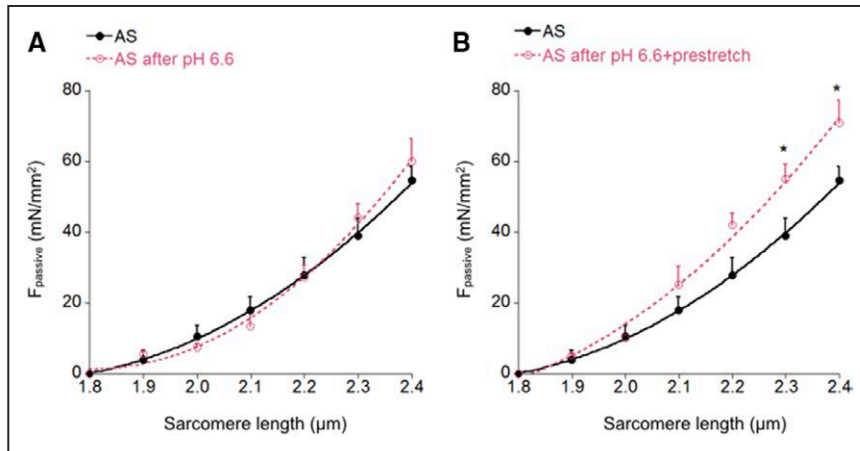


**Figure 5.** Effects of acidosis and prestretch on  $F_{\text{passive}}$  in single aortic stenosis (AS) myocytes. Incubating single AS cardiomyocytes in pH 6.6 did not change  $F_{\text{passive}}$  (A). Performing a prestretch to  $\approx 2.6 \mu\text{m}$  sarcomere length (SL) in pH 6.6 increased  $F_{\text{passive}}$  (B). \* $P < 0.05$  vs AS baseline.

### Cardiomyocyte Versus Extracellular Matrix Stiffness

High diastolic stiffness of failing human cardiomyocytes was a significant contributor to overall stiffness of LV myocardial strips of AS and DCM patients  $\leq 20\%$  stretch in AS and  $\leq 25\%$  stretch in DCM. Use of dissected myocardial strips precluded visualization of sarcomeres, and strip lengthening was, therefore, expressed as percentage of stretch with respect to slack length, that is, the minimal length at which  $F_{\text{passive}}$  started to develop (Figure 1). At 25% stretch, the contribution of cardiomyocyte stiffness to overall stiffness no longer differed between donor and AS cardiomyocytes but continued to differ between donor and DCM cardiomyocytes (Figure 3). This could relate to less constraint by the extracellular matrix in DCM despite raised collagen volume fraction in both AS and DCM.<sup>3,4</sup> The latter could be consistent with different distribution and homeostasis of myocardial fibrosis in AS and DCM: in DCM, there is focal replacement fibrosis, whereas in AS, there is diffuse reactive fibrosis<sup>3,4</sup> and, as reflected by plasma biomarker elevations, fibrinolytic mechanisms are present in DCM in contrast to mainly profibrotic mechanisms in AS.<sup>19</sup> These findings illustrate the importance of concentric versus eccentric remodeling for the constraint imposed by the extracellular matrix on the cardiomyocytes.

### Cardiomyocyte Stiffness and Titin Dephosphorylation

Altered cardiomyocyte stiffness can result from isoform shifts of the giant cytoskeletal protein titin, from post-translational modifications of titin such as phosphorylation,<sup>2,11,20–24</sup> formation of disulfide bonds,<sup>13</sup> carbonylation,<sup>25</sup> and s-glutathionylation<sup>14</sup> or from stretch-induced titin modification.<sup>15</sup> Because of higher expression of the compliant N2BA isoform in AS<sup>4</sup> and DCM,<sup>9,26</sup> titin isoform shifts do not contribute to the observed rise of cardiomyocyte stiffness observed in AS and DCM cardiomyocytes in the present study. Because of altered activity in failing myocardium of different kinases such as protein kinase A,<sup>2</sup> protein kinase C,<sup>23</sup> protein kinase G,<sup>21</sup> calcium/calmodulin-dependent kinase II,<sup>22</sup> and extracellular signal-regulated kinase,<sup>24</sup> altered phosphorylation of titin by these kinases was suspected to be involved in the raised stiffness of failing human cardiomyocytes. The present study confirms this involvement as it observed treatment with AP to raise diastolic stiffness in donor cardiomyocytes but not in AS and DCM cardiomyocytes (Figure 8). This implies a pre-existing imbalance of titin phosphorylation in AS and DCM cardiomyocytes with either reduced phosphorylation of sites that increase titin elasticity or increased phosphorylation of sites that decrease titin elasticity.

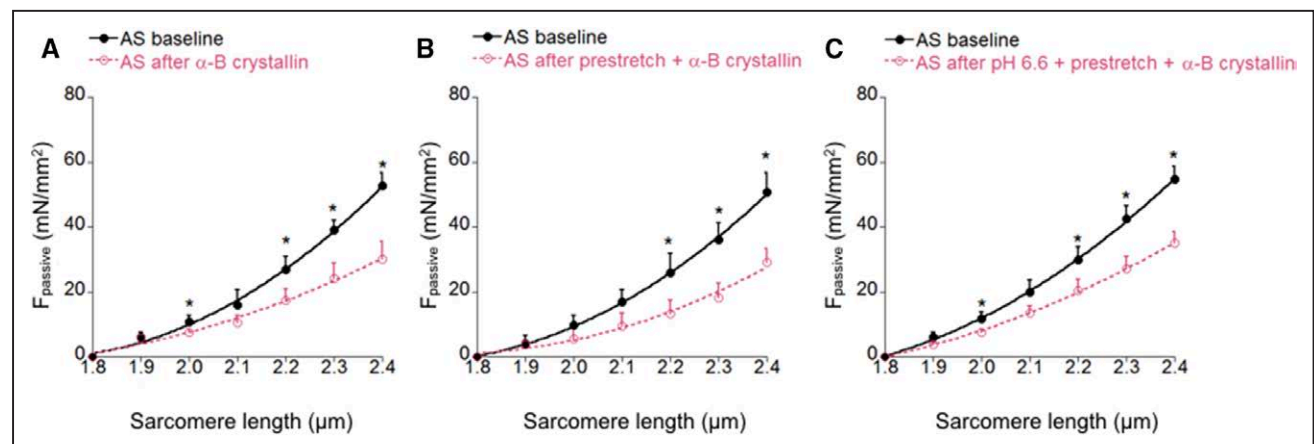


**Figure 6.** Effects of  $\alpha$ -B crystallin at baseline and after acidosis and prestretch on  $F_{\text{passive}}$  in single aortic stenosis (AS) cardiomyocytes. Incubation with  $\alpha$ -B crystallin decreased  $F_{\text{passive}}$  significantly (A). In single AS cardiomyocytes that underwent prestretch alone (B) or a prestretch in combination with pH 6.6 (C),  $\alpha$ -B crystallin also decreased  $F_{\text{passive}}$  significantly. \* $P < 0.05$  vs AS baseline.

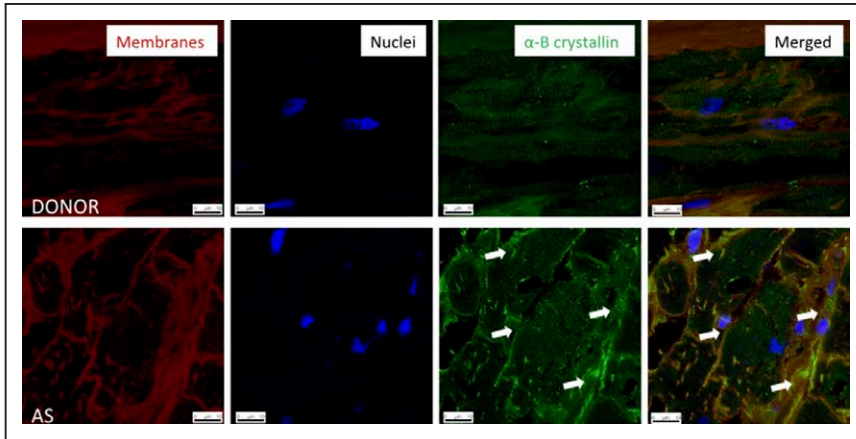


**Figure 7.** Confocal laser microscopy for  $\alpha$ -B crystallin in donor and aortic stenosis (AS). Confocal laser microscopic images were obtained from left ventricular (LV) myocardium of donor and AS patients with immunohistochemical visualization of cell membranes (A), nuclei (B), and  $\alpha$ -B crystallin (C). In myocardium of AS patients, intensity of  $\alpha$ -B crystallin expression (C) was higher than in donor with visualization in the merged images (D) of subsarcolemmal aggregates especially in the vicinity of capillaries (white arrows).

Post-translational modifications of titin other than phosphorylation have recently been implicated in altered cardiomyocyte stiffness. These mechanisms include among others modification of the titin molecule induced by excessive physical stretch. A previous study indeed showed stretch-induced mechanical unfolding of immunoglobulin domains of titin to expose cryptic cysteines to S-glutathionylation, which interfered with the ability of titin to refold and left titin in a more extensible state.<sup>14</sup> In acidic pH, the reverse was observed, namely, a prestretch-induced reduction of titin extensibility.<sup>15</sup> This is especially relevant to failing myocardium, which is exposed to both high filling pressures and jeopardized coronary perfusion. The present study, therefore, imposed prestretch and acidic pH on failing human cardiomyocytes.

### Cardiomyocyte Stiffness and Prestretch

In the present study, cardiomyocytes were subjected to a prestretch protocol, which consisted of a 15-minute stretch period at 2.6  $\mu\text{m}$  followed by a 5-minute stabilization period at slack length. This prestretch protocol was executed in pH 6.6 in donor, AS, and DCM cardiomyocytes. After dephosphorylation with AP, exposure to prestretch caused an upward shift of the diastolic  $F_{\text{passive}}-\text{SL}$  relations in AS and DCM cardiomyocytes and a further upward shift of the diastolic  $F_{\text{passive}}-\text{SL}$  relation in donor cardiomyocytes (Figure 4). The identical position of all diastolic  $F_{\text{passive}}-\text{SL}$  relations after prestretch argues in favor of previous stretch-induced damage being involved in the baseline elevation of diastolic stiffness of AS and DCM cardiomyocytes. The prestretch-induced upward shift of the diastolic  $F_{\text{passive}}-\text{SL}$  relations in AS and

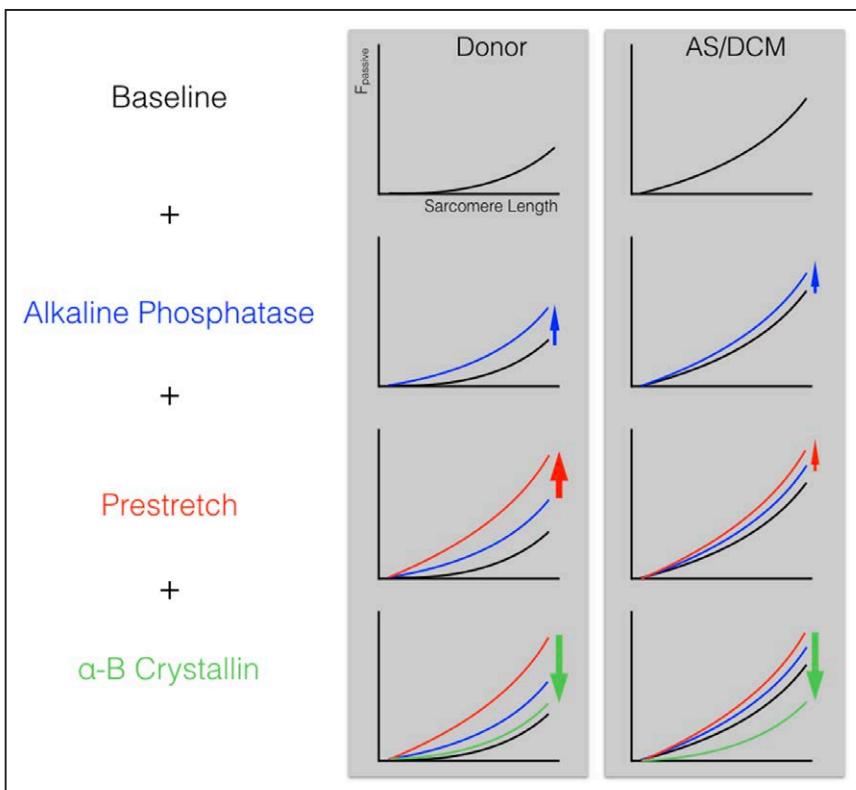


**Figure 8.** Diagram showing respective responses of donor and aortic stenosis (AS)/dilated cardiomyopathy (DCM) cardiomyocytes to administration of alkaline phosphatase, prestretch, and  $\alpha$ -B crystallin.

DCM cardiomyocytes was indeed smaller than the prestretch-induced upward shift of the diastolic  $F_{\text{passive}}$ -SL relation in donor cardiomyocytes (Figure 8). This yielded an identical position of all diastolic  $F_{\text{passive}}$ -SL relations because in AS and DCM cardiomyocytes, a smaller shift was superimposed on baseline stretch-induced damage, whereas in donor cardiomyocytes, prestretch elicited a larger shift because of absent baseline stretch-induced damage.

The origin of the baseline stretch-induced damage in AS and DCM cardiomyocytes is uncertain and could relate to external stretch on cardiomyocytes or to internal stretch within cardiomyocytes. The former obviously relates to elevated LV filling pressures at rest or during exercise. The latter is consistent with either a modified Z-disc structure or with the previously observed widening of the Z-disc.<sup>27</sup> Z-disc widening results from reduced elasticity of cytoskeletal proteins,<sup>28,29</sup> which from both sides pull at and open up adjacent Z lines. In AS and DCM cardiomyocytes, internal stretch and stretch-induced damage could have resulted from the aforementioned imbalance of titin phosphorylation.

In contrast to a previous study,<sup>14</sup> separate imposition of pH 6.6 failed to induce an upward shift of the diastolic  $F_{\text{passive}}$ -SL relation (Figure 5A). The upward shift of the diastolic  $F_{\text{passive}}$ -SL relation after combined administration of prestretch and acidic pH, therefore, seemed to be solely related to preceding sarcomere stretch. Furthermore, omission of previous treatment with AP also did not influence the combined effect of prestretch and acidic pH (Figure 5B).

### Cardiomyocyte Stiffness and $\alpha$ -B Crystallin

Beneficial myocardial effects of  $\alpha$ -B crystallin were previously reported in ischemia-reperfusion experiments<sup>30,31</sup> and attributed to interaction between  $\alpha$ -B crystallin and titin.<sup>16,32</sup> Recently, the small heat shock proteins HSP27 and  $\alpha$ -B crystallin were shown to protect cardiomyocytes against stretch-induced damage in acidic pH.<sup>15</sup> In these experiments, administration of small heat shock proteins to donor cardiomyocytes corrected the combined effects of prestretch and acidic pH on the diastolic  $F_{\text{passive}}$ -SL relation. This result was confirmed in the present study (Figure 4). The present study also administered  $\alpha$ -B crystallin to AS and DCM cardiomyocytes. In contrast to donor cardiomyocytes,  $\alpha$ -B crystallin not only corrected the combined effects of prestretch and acidic pH but also reversed the baseline upward displacement of the diastolic  $F_{\text{passive}}$ -SL relation (Figure 8). This finding was consistent with baseline involvement of previous stretch-induced titin damage in AS and DCM cardiomyocytes and was confirmed in a separate series of experiments, in which  $\alpha$ -B crystallin shifted the diastolic  $F_{\text{passive}}$ -SL relation downward without any previous or concomitant intervention (Figure 6). In these experiments, the magnitude of the downward displacement of the diastolic  $F_{\text{passive}}$ -SL relation was similar in the absence (Figure 6A) or presence of foregoing interventions (Figure 6B and 6C).

In AS and DCM cardiomyocytes,  $\alpha$ -B crystallin lowered diastolic stiffness well below baseline values as previously reported after administration of protein kinase A or protein kinase G PKA or PKG.<sup>2,4,20,21</sup> This supports overlapping

effects of titin phosphorylation and stretch-induced titin aggregation possibly because of pre-existing stretch-induced titin aggregation obstructing phosphorylation at sites that specifically increase titin elasticity. This finding has important therapeutic implications as it implies limited efficacy of drugs that increase PKA or PKG activity for treatment of diastolic LV dysfunction related to high cardiomyocyte stiffness and could relate to the failure of dobutamine to improve diastolic LV dysfunction<sup>33</sup> and of phosphodiesterase 5 inhibitors to improve exercise tolerance or hemodynamics in HFPEF.<sup>34,35</sup>

The present study observed upregulation and subsarcolemmal localization of  $\alpha$ -B crystallin in AS and DCM cardiomyocytes. Because of the close vicinity of capillaries (white arrows in Figure 7), the localization of  $\alpha$ -B crystallin in subsarcolemmal aggregates was consistent with signals from the microvascular endothelium being involved in their formation. The subsarcolemmal localization also suggested that endogenous  $\alpha$ -B crystallin was diverted from the sarcomeres and therefore failed to exert its protective action on titin distensibility, which was, however, restored after administration of exogenous  $\alpha$ -B crystallin. The latter finding supports future therapeutic efforts to raise concentration of  $\alpha$ -B crystallin in failing myocardium through direct administration of  $\alpha$ -B crystallin, through administration of  $\alpha$ -B crystallin analogues or through administration of heat shock protein-inducing drugs such as geranylgeranylacetone or NYK9354.

### Limitations

The limited size of donor and patient populations reduced statistical power and precision of estimates. The study failed to address titin isoform shifts in the AS and DCM samples and presumed larger expression of the compliant N2BA titin isoform in both conditions based on previous evidence obtained in the author's<sup>3,4</sup> and in other<sup>9</sup> laboratories. A potential contribution of altered titin isoform expression could, therefore, not be excluded. Furthermore, the effects of AP administration on  $F_{\text{passive}}$  in donor, AS, and DCM samples were not confirmed by measures of overall titin phosphorylation.

### Conclusions

High cardiomyocyte stiffness significantly contributed to overall myocardial stiffness in AS and DCM. High cardiomyocyte stiffness resulted from titin phosphorylation failing to improve cardiomyocyte stiffness and from previous stretch-induced aggregation of titin, both of which were corrected by administration of  $\alpha$ -B crystallin. Diastolic LV dysfunction in heart failure could, therefore, benefit from treatment with  $\alpha$ -B crystallin.

### Sources of Funding

This study was supported by grants from the European Commission (FP7-Health-2010; MEDIA-261409), from CardioVasculaire Onderzoek Nederland (CVON: ARENA, RECONNECT, and EARLY-HFPEF).

### Disclosures

None.



## References

- Borlaug BA, Paulus WJ. Heart failure with preserved ejection fraction: pathophysiology, diagnosis, and treatment. *Eur Heart J*. 2011;32:670–679. doi: 10.1093/eurheartj/ehq426.
- Borbély A, van der Velden J, Papp Z, Bronzwaer JG, Edes I, Stienen GJ, Paulus WJ. Cardiomyocyte stiffness in diastolic heart failure. *Circulation*. 2005;111:774–781. doi: 10.1161/01.CIR.0000155257.33485.6D.
- van Heerebeek L, Borbély A, Niessen HW, Bronzwaer JG, van der Velden J, Stienen GJ, Linke WA, Laarman GJ, Paulus WJ. Myocardial structure and function differ in systolic and diastolic heart failure. *Circulation*. 2006;113:1966–1973. doi: 10.1161/CIRCULATIONAHA.105.587519.
- Falcão-Pires I, Hamdani N, Borbély A, Gavina C, Schalkwijk CG, van der Velden J, van Heerebeek L, Stienen GJ, Niessen HW, Leite-Moreira AF, Paulus WJ. Diabetes mellitus worsens diastolic left ventricular dysfunction in aortic stenosis through altered myocardial structure and cardiomyocyte stiffness. *Circulation*. 2011;124:1151–1159. doi: 10.1161/CIRCULATIONAHA.111.025270.
- Granzier HL, Irving TC. Passive tension in cardiac muscle: contribution of collagen, titin, microtubules, and intermediate filaments. *Biophys J*. 1995;68:1027–1044. doi: 10.1016/S0006-3495(95)80278-X.
- Hudson B, Hidalgo C, Saripalli C, Granzier H. Hyperphosphorylation of mouse cardiac titin contributes to transverse aortic constriction-induced diastolic dysfunction. *Circ Res*. 2011;109:858–866. doi: 10.1161/CIRCRESAHA.111.246819.
- Chung CS, Hutchinson KR, Methawasini M, Saripalli C, Smith JE 3rd, Hidalgo CG, Luo X, Labeit S, Guo C, Granzier HL. Shortening of the elastic tandem immunoglobulin segment of titin leads to diastolic dysfunction. *Circulation*. 2013;128:19–28. doi: 10.1161/CIRCULATIONAHA.112.001268.
- Hamdani N, Fransen C, Lourenço A, Falcão-Pires I, Fontoura D, Leite S, Plettig L, López B, Ottenheijm CA, Becher PM, González A, Tschöpe C, Díez J, Linke WA, Leite-Moreira AF, Paulus WJ. Myocardial titin hypophosphorylation importantly contributes to heart failure with preserved ejection fraction in a rat metabolic risk model. *Circ Heart Fail*. 2013;6:1239–1249. doi: 10.1161/CIRCHEARTFAILURE.113.000539.
- Nagueh SF, Shah G, Wu Y, Torre-Amione G, King NM, Lahmers S, Witt CC, Becker K, Labeit S, Granzier HL. Altered titin expression, myocardial stiffness, and left ventricular function in patients with dilated cardiomyopathy. *Circulation*. 2004;110:155–162. doi: 10.1161/01.CIR.0000135591.37759.AF.
- Zile MR, Baicu CF, Ikonomidis JS, Stroud RE, Nietert PJ, Bradshaw AD, Slater R, Palmer BM, Van Buren P, Meyer M, Redfield MM, Bull DA, Granzier HL, LeWinter MM. Myocardial stiffness in patients with heart failure and a preserved ejection fraction: contributions of collagen and titin. *Circulation*. 2015;131:1247–1259. doi: 10.1161/CIRCULATIONAHA.114.013215.
- Linke WA, Hamdani N. Gigantic business: titin properties and function through thick and thin. *Circ Res*. 2014;114:1052–1068. doi: 10.1161/CIRCRESAHA.114.301286.
- Sharma K, Kass DA. Heart failure with preserved ejection fraction: mechanisms, clinical features, and therapies. *Circ Res*. 2014;115:79–96. doi: 10.1161/CIRCRESAHA.115.302922.
- Grützner A, Garcia-Manyes S, Kötter S, Badilla CL, Fernandez JM, Linke WA. Modulation of titin-based stiffness by disulfide bonding in the cardiac titin N2-B unique sequence. *Biophys J*. 2009;97:825–834. doi: 10.1016/j.bpj.2009.05.037.
- Alegre-Cebollada J, Kosuri P, Giganti D, Eckels E, Rivas-Pardo JA, Hamdani N, Warren CM, Solaro RJ, Linke WA, Fernández JM. S-glutathionylation of cryptic cysteines enhances titin elasticity by blocking protein folding. *Cell*. 2014;156:1235–1246. doi: 10.1016/j.cell.2014.01.056.
- Kötter S, Unger A, Hamdani N, Lang P, Vorgerd M, Nagel-Steger L, Linke WA. Human myocytes are protected from titin aggregation-induced stiffening by small heat shock proteins. *J Cell Biol*. 2014;204:187–202. doi: 10.1083/jcb.201306077.
- Zhu Y, Bogomolovas J, Labeit S, Granzier H. Single molecule force spectroscopy of the cardiac titin N2B element: effects of the molecular chaperone  $\alpha$ B-crystallin with disease-causing mutations. *J Biol Chem*. 2009;284:13914–13923. doi: 10.1074/jbc.M809743200.
- Borbély A, Falcao-Pires I, van Heerebeek L, Hamdani N, Edes I, Gavina C, Leite-Moreira AF, Bronzwaer JG, Papp Z, van der Velden J, Stienen GJ, Paulus WJ. Hypophosphorylation of the Stiff N2B titin isoform raises cardiomyocyte resting tension in failing human myocardium. *Circ Res*. 2009;104:780–786. doi: 10.1161/CIRCRESAHA.108.193326.
- Wang X, Robbins J. Heart failure and protein quality control. *Circ Res*. 2006;99:1315–1328. doi: 10.1161/01.RES.0000252342.61447.a2.
- Spinale FG, Janicki JS, Zile MR. Membrane-associated matrix proteolysis and heart failure. *Circ Res*. 2013;112:195–208. doi: 10.1161/CIRCRESAHA.112.266882.
- Fukuda N, Wu Y, Nair P, Granzier HL. Phosphorylation of titin modulates passive stiffness of cardiac muscle in a titin isoform-dependent manner. *J Gen Physiol*. 2005;125:257–271. doi: 10.1085/jgp.200409177.
- Krüger M, Kötter S, Grützner A, Lang P, Andresen C, Redfield MM, Butt E, dos Remedios CG, Linke WA. Protein kinase G modulates human myocardial passive stiffness by phosphorylation of the titin springs. *Circ Res*. 2009;104:87–94. doi: 10.1161/01.CIRCRESAHA.108.184408.
- Hamdani N, Krysiak J, Kreuzer MM, Neef S, Dos Remedios CG, Maier LS, Krüger M, Backs J, Linke WA. Crucial role for Ca<sup>2+</sup>/calmodulin-dependent protein kinase-II in regulating diastolic stress of normal and failing hearts via titin phosphorylation. *Circ Res*. 2013;112:664–674. doi: 10.1161/CIRCRESAHA.111.300105.
- Hidalgo C, Hudson B, Bogomolovas J, Zhu Y, Anderson B, Greaser M, Labeit S, Granzier H. PKC phosphorylation of titin's PEVK element: a novel and conserved pathway for modulating myocardial stiffness. *Circ Res*. 2009;105:631–638, 17 p following 638. doi: 10.1161/CIRCRESAHA.109.198465.
- Raskin A, Lange S, Banares K, Lyon RC, Ziesenis A, Lee LK, Yamazaki KG, Granzier HL, Gregorio CC, McCulloch AD, Omens JH, Sheikh F. A novel mechanism involving four-and-a-half LIM domain protein-1 and extracellular signal-regulated kinase-2 regulates titin phosphorylation and mechanics. *J Biol Chem*. 2012;287:29273–29284. doi: 10.1074/jbc.M112.372839.
- Balogh A, Santer D, Pásztor ET, Tóth A, Czurgiga D, Podesser BK, Trescher K, Jaquet K, Erdodi F, Edes I, Papp Z. Myofilament protein carbonylation contributes to the contractile dysfunction in the infarcted LV region of mouse hearts. *Cardiovasc Res*. 2014;101:108–119. doi: 10.1093/cvr/cvt236.
- Makarenko I, Opitz CA, Leake MC, Neagoe C, Kulke M, Gwathmey JK, del Monte F, Hajjar RJ, Linke WA. Passive stiffness changes caused by upregulation of compliant titin isoforms in human dilated cardiomyopathy hearts. *Circ Res*. 2004;95:708–716. doi: 10.1161/01.RES.0000143901.37063.2f.
- van Heerebeek L, Hamdani N, Handoko ML, Falcao-Pires I, Musters RJ, Kupreishvili K, Ijsselmuiden AJ, Schalkwijk CG, Bronzwaer JG, Diamant M, Borbély A, van der Velden J, Stienen GJ, Laarman GJ, Niessen HW, Paulus WJ. Diastolic stiffness of the failing diabetic heart: importance of fibrosis, advanced glycation end products, and myocyte resting tension. *Circulation*. 2008;117:43–51. doi: 10.1161/CIRCULATIONAHA.107.728550.
- Hoshijima M. Mechanical stress-strain sensors embedded in cardiac cytoskeleton: Z disk, titin, and associated structures. *Am J Physiol Heart Circ Physiol*. 2006;290:H1313–H1325. doi: 10.1152/ajpheart.00816.2005.
- Witt CC, Burkart C, Labeit D, McNabb M, Wu Y, Granzier H, Labeit S. Nebulin regulates thin filament length, contractility, and Z-disk structure in vivo. *EMBO J*. 2006;25:3843–3855. doi: 10.1038/sj.emboj.7601242.
- Morrison LE, Whittaker RJ, Klepper RE, Wawrousek EF, Glembofski CC. Roles for  $\alpha$ B-crystallin and HSPB2 in protecting the myocardium from ischemia-reperfusion-induced damage in a KO mouse model. *Am J Physiol Heart Circ Physiol*. 2004;286:H847–H855. doi: 10.1152/ajpheart.00715.2003.
- Kadono T, Zhang XQ, Srinivasan S, Ishida H, Barry WH, Benjamin IJ. CRYAB and HSPB2 deficiency increases myocyte mitochondrial permeability transition and mitochondrial calcium uptake. *J Mol Cell Cardiol*. 2006;40:783–789. doi: 10.1016/j.yjmcc.2006.03.003.
- Golenhofen N, Arbeiter A, Koob R, Drenckhahn D. Ischemia-induced association of the stress protein  $\alpha$ B-crystallin with I-band portion of cardiac titin. *J Mol Cell Cardiol*. 2002;34:309–319. doi: 10.1006/jmcc.2001.1513.
- Chattoopadhyay S, Alamgir MF, Nikitin NP, Rigby AS, Clark AL, Cleland JG. Lack of diastolic reserve in patients with heart failure and normal ejection fraction. *Circ Heart Fail*. 2010;3:35–43. doi: 10.1161/CIRCHEARTFAILURE.108.824888.
- Redfield MM, Chen HH, Borlaug BA, Semigran MJ, Lee KL, Lewis G, LeWinter MM, Rouleau JL, Bull DA, Mann DL, Deswal A, Stevenson LW, Givertz MM, Ofili EO, O'Connor CM, Felker GM, Goldsmith SR,

Bart BA, McNulty SE, Ibarra JC, Lin G, Oh JK, Patel MR, Kim RJ, Tracy RP, Velazquez EJ, Anstrom KJ, Hernandez AF, Mascette AM, Braunwald E; RELAX Trial. Effect of phosphodiesterase-5 inhibition on exercise capacity and clinical status in heart failure with preserved ejection fraction: a randomized clinical trial. *JAMA*. 2013;309:1268–1277. doi: 10.1001/jama.2013.2024.

35. Hoendermis ES, Liu LC, Hummel YM, van der Meer P, de Boer RA, Berger RM, van Veldhuisen DJ, Voors AA. Effects of sildenafil on invasive haemodynamics and exercise capacity in heart failure patients with preserved ejection fraction and pulmonary hypertension: a randomized controlled trial. *Eur Heart J*. 2015;36:2565–2573. doi: 10.1093/eurheartj/ehv336.

### CLINICAL PERSPECTIVE

High diastolic left ventricular stiffness results from myocardial collagen deposition and reduced distensibility of cardiomyocytes. Distensibility of cardiomyocytes is controlled by the giant cytoskeletal protein titin, whose elasticity is altered by isoform shifts, phosphorylation, and oxidative or prestretch-induced damage. The latter was recently shown to react favorably to administration of small heat shock proteins such as  $\alpha$ -B crystallin. The present study assesses: (1) the relative contributions of collagen and titin to the raised diastolic stiffness of left ventricular myocardial strips in aortic stenosis (AS) and dilated cardiomyopathy (DCM); (2) the importance of titin phosphorylation and titin prestretch for distensibility of cardiomyocytes isolated from explanted donor hearts, AS, and DCM patients; and (3) the effects of  $\alpha$ -B crystallin on cardiomyocyte distensibility. The study demonstrates both collagen and titin to contribute to the raised diastolic stiffness in AS and DCM. Dephosphorylation of titin raises passive tension ( $F_{\text{passive}}$ ) in donors but not in AS and DCM. The inability of phosphorylation status to modify  $F_{\text{passive}}$  in AS and DCM could explain the failure to correct high diastolic left ventricular stiffness with drugs that raise protein kinase G activity. A 15-minute prestretch period raises  $F_{\text{passive}}$  to a similar level in donors, AS, and DCM. Subsequent administration of  $\alpha$ -B crystallin lowers  $F_{\text{passive}}$  to baseline in donor and to lower than baseline in AS and DCM. This finding supports presence of prestretch-induced titin damage in AS and DCM and suggests  $\alpha$ -B crystallin analogues or heat shock protein-inducing drugs to be effective against high diastolic left ventricular stiffness.

**$\alpha$ -B Crystallin Reverses High Diastolic Stiffness of Failing Human Cardiomyocytes**  
Constantijn Franssen, Jeroen Kole, René Musters, Nazha Hamdani and Walter J. Paulus

*Circ Heart Fail.* 2017;10:e003626

doi: 10.1161/CIRCHEARTFAILURE.116.003626

*Circulation: Heart Failure* is published by the American Heart Association, 7272 Greenville Avenue, Dallas, TX 75231

Copyright © 2017 American Heart Association, Inc. All rights reserved.

Print ISSN: 1941-3289. Online ISSN: 1941-3297

The online version of this article, along with updated information and services, is located on the World Wide Web at:

<http://circheartfailure.ahajournals.org/content/10/3/e003626>

**Permissions:** Requests for permissions to reproduce figures, tables, or portions of articles originally published in *Circulation: Heart Failure* can be obtained via RightsLink, a service of the Copyright Clearance Center, not the Editorial Office. Once the online version of the published article for which permission is being requested is located, click Request Permissions in the middle column of the Web page under Services. Further information about this process is available in the [Permissions and Rights Question and Answer](#) document.

**Reprints:** Information about reprints can be found online at:  
<http://www.lww.com/reprints>

**Subscriptions:** Information about subscribing to *Circulation: Heart Failure* is online at:  
<http://circheartfailure.ahajournals.org/subscriptions/>